Dalton Transactions

Ion-Pairing in Polyoxometalate Chemistry: Impact of Fully Hydrated Alkali Metal Cations on Properties of the Keggin $[PW_{12}O_{40}]^{3-}$ Anion

Journal:	*Dalton Transactions*
Manuscript ID	DT-ART-06-2020-002239.R1
Article Type:	Paper
Date Submitted by the Author:	14-Jul-2020
Complete List of Authors:	Kaledin, Alexey; Emory University, Cherry L. Emerson Center for Scientific Computation Yin, Qiushi; Emory University Hill, Craig; Emory University Lian, Tianquan; Emory University Musaev, D.; Emory University

Ion-Pairing in Polyoxometalate Chemistry: Impact of Fully Hydrated Alkali Metal Cations on Properties of the Keggin $[PW_{12}O_{40}]^{3-}$ Anion

Alexey L. Kaledin,[1] Qiushi Yin,[2] Craig L. Hill,[1,2] Tianquan Lian,[1,2] and Djamaladdin G. Musaev[1,2,*]

[1] *Emerson Center for Scientific Computation, Emory University, Atlanta, Georgia 30322 USA*
[2] *Department of Chemistry, Emory University, Atlanta, Georgia 3032 USA*

Abstract

The counterions of polyoxometalates (POMs) impact properties and applications of this growing class of inorganic clusters. Here, we used density functional theory (DFT) to elucidate the impact of fully hydrated alkali metal cations on the geometry, electronic structure, and chemical properties of the polyoxotungstate anion $[PW_{12}O_{40}]^{3-}$. The calculations show that the HOMO of the free anion $[PW_{12}O_{40}]^{3-}$ is a linear combination of the 2*p* AOs of the bridging oxygens, and the first few LUMOs are the 5*d* orbitals of the tungsten atoms. The $S_0 \rightarrow S_1$ electron excitation, near 3 eV, is associated with the O(2*p*) $\rightarrow$ W(5*d*) transition. Anion/cation complexation leads to formation of $[PW_{12}O_{40}]^{3-}[M^+(H_2O)_{16}]_3$ ion-pair complexes, where with the increase of atomic number of M, the $M^+(H_2O)_{16}$ cluster releases several water molecules and interacts strongly with the polyoxometalate anion. For M = Li, Na and K, $[PW_{12}O_{40}]^{3-}[M^+(H_2O)_{16}]_3$ is characterized as a "hydrated" ion-pair complex. However, for M = Rb and Cs, it is a "contact" ion-pair complex, where the strong anion-cation interaction makes it a better electron acceptor than one of the "hydrated" ion-pair complexes. Remarkably, the electronic excitations in the visible part of the absorption spectrum of these complexes are predominantly solvent-to-POM charge transfer transitions (i.e. intermolecular CT). The ratio of the number of intermolecular charge transfer transitions to the number of O(2*p*)-to-W(5*d*) valence (i.e. intramolecular) transitions increases with the increasing atomic number of the alkali metals.

Introduction

Ion-pairing plays critical a role in many areas of chemical, physical, biological and materials sciences. It generates necessary chemical space to stabilize exotic structural motifs with unmatched properties, impacts reactivity of catalytic active species to drive highly selective chemical transformations, promotes critical intermolecular charge transfer (CT) in biologically vital processes, drives optical and electronic properties of industrially critical materials, and more. For example, ion-pairing influences nearly all properties of the growing exotic class of transition-metal oxygen-anion clusters (polyoxometalates or "POMs").[1-5] Briefly, cation-POM ion-pairing is shown to be critical for rates of redox processes,[6-13] acid-base behavior,[14-17] self assembly,[18,19] solubilities[20,21], magnetic properties,[21,5] biological activities,[22] and speciation,[23] among other fundamental properties, of highly anionic polyoxometalates. While the counter cations are frequently written in POM formulas and noted in X-ray structures, their specific roles in redox, acid-base and other fundamental properties of highly anionic POMs, as well as the nature of highly charged metal-oxide anions, are not well analyzed.[24] The current POM-related literature divides the existing hydrated counter cation – POM ion-parings into three categories: (a) the hydrated counter cations *neither* directly bonded (i.e. a POM oxygen is not directly ligated by the cation)

nor hydrogen-bonded to a POM oxygen; this type of ion-pairing is called an "outer sphere" ion-pairing, (b) the hydrated counter cations are hydrogen bonded to a POM oxygen, which could be called and "hydrogen-bonded" ion-pairing,[25] and (c) the counter cations (CC) directly bonded to a POM oxygen (i.e. via the CC-O-M bonding motive).[26] This category is referred to as "contact" ion pairs. Since quantifying ion-pairing and identifying the impact of counter cation on stability, structural motifs and reactivity of the highly anionic POMs are challenging and important tasks, in this paper we examine the geometries and electronic structure of the alkali metal salts of the most studied heteropolytungstate, $[PW_{12}O_{40}]^{3-}$, using density functional theory. These calculations clarify the key frontier orbitals, electronic transitions and potentials in these ubiquitous $[PW_{12}O_{40}]^{3-}[M^{+}(H_2O)_n]_3$ complexes, where M = Li, Na, K, Cs and Rb. The findings herein should be fairly general for other POMs and particularly extrapolatable to the myriads of polytungstates.

2. Computational methods

The electronic structure calculations were carried out at the M06L density functional level,[27] which has previously been used by us in describing the reactivity of the negatively charged Lindqvist ion in the presence of water molecules and Cs^+ ions (used as counter cations).[28,29] Following that work, here, we utilized the 6-31++G(d,p) basis sets[30] for P, O and H atoms, D95V for Li,[31] and the LANL2DZ ECPs with the corresponding basis sets for W, Na, K, Rb and Cs.[32] The excited states of the studied molecules were calculated with the time-dependent (TD) DFT[33] using the density functional and basis sets above. The effects of bulk aqueous solution were approximated at the level of the polarizable continuum model (PCM).[34-35] All calculations were performed using Gaussian 09 (Revision E.01) quantum chemical software package.[36]

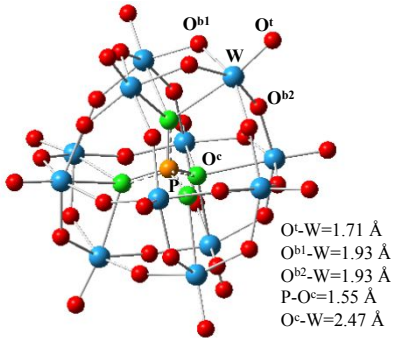

Figure 1. The calculated structure and important geometry parameters of the polyoxometalate anion $[PW_{12}O_{40}]^{3-}$ at its ground electronic state, S_0 (see Supporting Materials for more details). The terminal, bridging and central (i.e. of PO_4-unit) oxygens are labeled as O^t, O^{b1}, and O^c, respectively. The oxygens of the PO_4-unit are green, while the P and W atoms yellow-orange and blue, respectively.

3. Results and discussion

3.1. Properties of the $[PW_{12}O_{40}]^{3-}$ anion

The geometry and electronic structure of the anion $[PW_{12}O_{40}]^{3-}$ have been subject of several previous computational and experimental studies.[25,37-39] Our findings (see Figure 1 and Supporting Materials) are fully consistent with the previously reported data. The calculated W=O^t, W-O^b, and W-O^c bond distances are 1.71, 1.93 and 2.47 Å, respectively. In a simplified picture, the electron configuration of this anion derives from the fully oxidized tungstens W^{6+} ($5d^0 6s^0$), *p*-shell filled oxygen O^{2-}anions, and a $[PO_4]^{3-}$ unit. The calculation, in fact, assigns O^t a -0.64 |e| charge, and further differentiates the bridging oxygens into O^{b1} and O^{b2}, with a -1.04 |e| and -1.21 |e| charges, respectively.

Analysis of the frontier orbitals reveals a HOMO-LUMO gap of 2.99 eV and reflects the simple ionic picture, with the HOMOs being linear combinations of the $O^{b1}(2p)$ and $O^{b2}(2p)$ AOs and the first few LUMOs being primarily W(5*d*) orbitals, as seen in Figure 2. The low potential of the first

5 LUMOs, -4.1 to -3.7 eV, points to a strong electron affinity of the anion $[PW_{12}O_{40}]^{3-}$, which is consistent with the available experiments.[37] The lowest energy electron excitations, with the $S_0 \rightarrow S_1$ being near 3 eV, are valence O(2*p*) → W(5*d*) transitions.

A more complete picture of the excited states is summarized in Figure 3, where we present the UV-VIS spectrum calculated as vertical excitation energies, with dipole intensities, at the S_0 global minimum. The leading singlet states, S_n for n=1-73, are all dark states since the HOMO → LUMO orbitals involved in these transitions possess quasi-spherical symmetry, resulting in near cancellation of the <HOMO|μ|LUMO> matrix elements, where μ is the dipole operator.

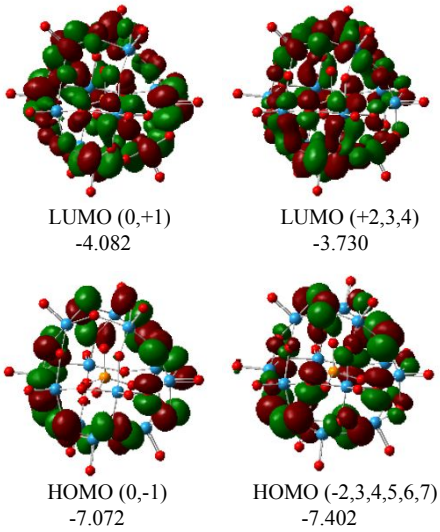

Figure 2. Frontier MOs of the Keggin $[PW_{12}O_{40}]^{3-}$ ion with their energies (in eV). The eight highest occupied and five lowest virtual MOs are combined in degenerate groups: LUMO (0,+1) form a doubly degenerate pair followed by LUMO (+2,3,4) as a triply degenerate group, all dominated by W(5*d*) orbitals. HOMO (0,-1) form a doubly degenerate pair with HOMO (-2,3,4,5,6,7) forming a six-fold degenerate group, characterized by $O^b(2p)$.

The first transitions with strong intensity show up as band **A**, containing the states $S_{74\text{-}80}$ and centered around 3.9 eV; they are mostly $O^b(2p) \rightarrow W(5d)/O^b(2p)$ and $O^t(2p) \rightarrow W(5d)/O^b(2p)$ transitions involving occupied orbitals with well-defined asymmetry (see Supporting Materials for details). Band **A** is followed by a stronger band **B**, made up of two state groups $S_{135\text{-}137}$ and $S_{164\text{-}166}$ and centered at 4.3 eV; it is dominated by $O^t(2p) \rightarrow W(5d)/O^b(2p)$ and $O^b(2p) \rightarrow W(5d)/O^t(2p)$ transitions. We note that the direct contribution from the triplet states is ignored in the spectrum due to the lack of spin-orbit mixing in present calculations, but it is expected to broaden both the optically active singlet bands. We note the large density of triplet states in the 3.6-4.4 range eV. A further role of the triplets is their expected involvement in non-radiative decay of the highly excited bright singlets (in bands **A** and **B**) to the lowest energy optically dark S_1/T_1 pair, which is a candidate state for electron transfer to an electron acceptor.

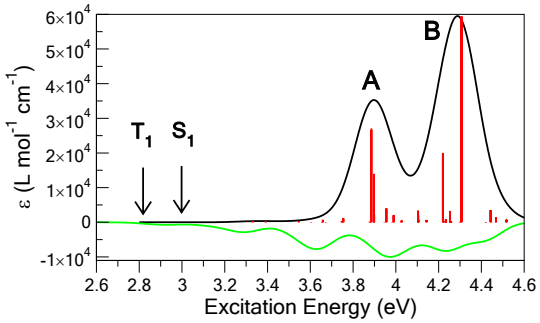

Figure 3. UV-VIS (vertical) spectrum of $[PW_{12}O_{40}]^{3-}$ based on the first 200 singlet states (red sticks), convoluted with a Gaussian lineshape (black curve). The density of triplet states is represented by the inverted green curve.

In the presence of liquid water and alkali metal cations, (M^+ = Li^+, Na^+, K^+, Rb^+, and Cs^+), the $[PW_{12}O_{40}]^{3-}$ anion is expected to be fully solvated and charge-balanced by the hydrated counter cations to form $[PW_{12}O_{40}]^{3-}[M^+(H_2O)_n]_3$ complexes. However, key details of the $[PW_{12}O_{40}]^{3-}$-$[M^+(H_2O)_n]_3$ interaction and structural motifs of the $[PW_{12}O_{40}]^{3-}[M^+(H_2O)_n]_3$ complexes remain unresolved.

3.2. The water clusters of alkali-metal cations

In this paper, we intend to elucidate the nature of the cation-anion interaction and key structural features of the common polyoxometalate complex in water, $[PW_{12}O_{40}]^{3-}[M^+(H_2O)_n]_3$. To this end, we first determine the number of water molecules needed to solvate each alkali-metal cation (M^+ = Li^+, Na^+, K^+, Rb^+, and Cs^+) in an *aqueous* solution. In our calculations of the $M^+(H_2O)_n$ clusters, we fully saturate the first solvation shell of the cation by stepwise increasing the number of closely coordinated water molecules to the metal cation. We found that the first solvation shell of Li^+, Na^+, K^+, and Cs^+ cations contains a maximum of 6, 7, 8, and 12 closely coordinated water molecules, respectively. The first solvation shell of the Rb^+ cation includes 8 closely coordinated water molecules and four slightly weaker coordinated water molecules, therefore, its coordination number is described as being anywhere between 8 and 12. These findings are consistent with previously reported computational and well-known experimental[40] data. For example, recent high-level electronic structure calculations on Na^+/water clusters confirm that the first solvation shell of Na^+ contains at least 6 water molecules.[41] However, in the present study of the $[PW_{12}O_{40}]^{3-}[M^+(H_2O)_n]_3$ structures, to keep the alkali metal solvation spheres maximally similar, the same number of water molecules, *a total of sixteen*, was used for all our calculations (see Figure 4).

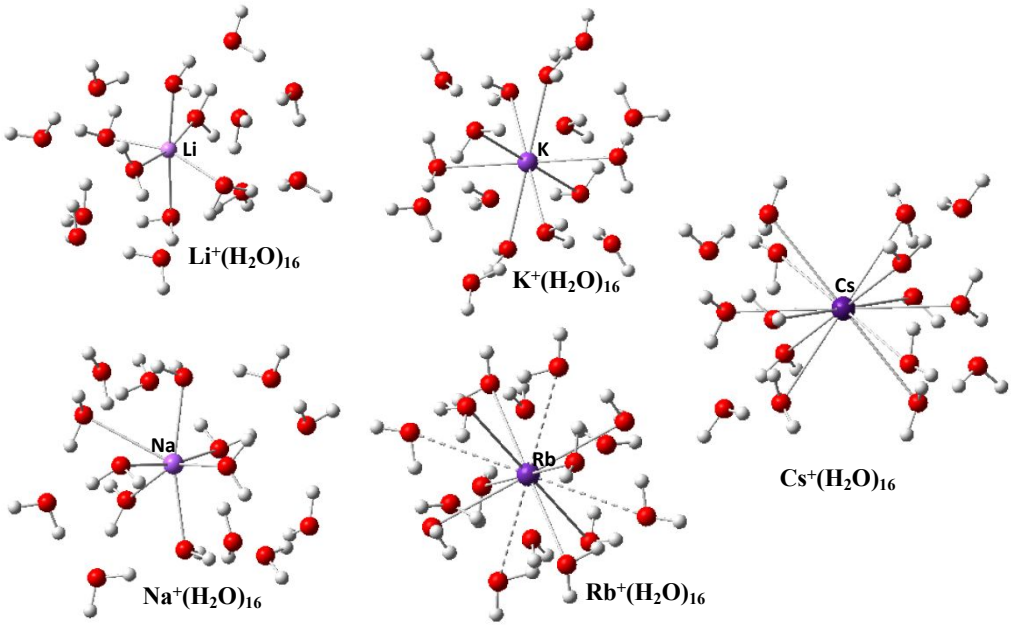

Figure 4. Counter cations of the hydrated metal clusters with 16 water molecules, i.e. $M^+(H_2O)_{16}$. The first solvation spheres are marked by solid metal-oxygen bonds: with 6 water molecules for M = Li, with 7 water molecules for M = Na, 8 water molecules for M = K, 8-12 water molecules for M = Rb, and 12 water molecules for M = Cs (see text). For all clusters, the water molecules assigned to the second solvation sphere are omitted.

We found that solvating the alkali metal cations by 16 water molecules is sufficient to provide a balanced description (*vide infra* for details). As one can see in Figure 4, the first solvation shell of each cation expands with the increasing atomic number of alkali metal. In Figure 5 we presented the radii of the cation hydration shells, which are assumed to be spherical, versus atomic number. As expected, the calculations show that the number of water molecules coordinated to the metal centers increases with increasing radius of the cation solvation shell. Similar values for the size of the first solvation shell were reported for the $Li^+(H_2O)_6$, $Na^+(H_2O)_6$, and $K^+(H_2O)_6$ at 2.0, 2.5 and

2.7 Å, respectively at the EFP/6-31+G* level of theory.[42] More recently, Wang and coworkers have reported ~2.5 Å Na-O bond distance in $Na^+(H_2O)_6$,[41] supporting the earlier EFP results.

The solvation of Rb^+ and Cs^+, using up to 9 water molecules, has been studied with MP2/6-31+G*, resulting in the respective metal-oxygen bond distances of ~3.1 and ~3.4 Å.[43] The binding energies of an outermost water molecule in the cluster, i.e. dehydration by a single water molecule $E[M^+(H_2O)_{16} \rightarrow M^+(H_2O)_{15} + H_2O\ ]$, are -15.5, -15.1, -12.8, -14.1 and -0.3 kcal/mol for M = Li, Na, K, Rb and Cs. In other words, the second solvation shell becomes "softer" with the increasing atomic radius, which implies that the heavier ions should donate a water to the negatively charged POM anion more readily than the lighter ones.

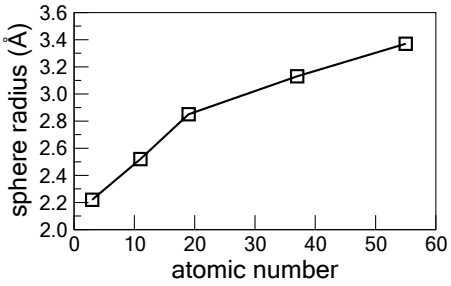

Figure 5. The first solvation sphere radius defined as the average M^+-OH_2 distance in the ion-water clusters $M^+(H_2O)_{16}$, where M=Li, Na, K, Rb, Cs.

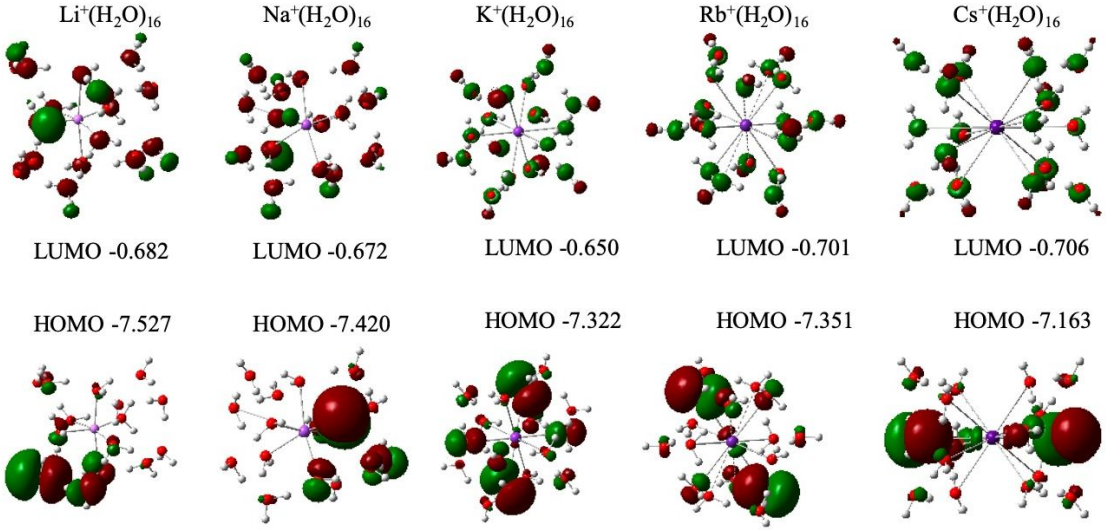

Figure 6. Frontier molecular orbitals of the five hydrated alkali ions; the MO energies are given in eV. Localization of the HOMOs is clearly visible in contrast to delocalization of the LUMOs.

Inspection of the frontier molecular orbitals of the hydrated cations, summarized in Figure 6, reveals a common picture. The HOMO of the $M^+(H_2O)_n$ clusters is a 2pπ lone-pair orbital that is localized on one (in Li, Na) or two (in K, Rb, Cs) of the water molecules in the second solvation shell, and the LUMO of these clusters is a 2pσ* antibonding orbital that is delocalized over all the water molecules of the cluster. The occupied MOs of the waters in the first solvation shell are spatially closer to the alkali metal cations and stabilized by the cation-water interactions. The LUMOs, on the other hand, are evidently not as affected by the presence of cations, and therefore involve all water molecules rather uniformly. The increasing atomic radius of the alkali metal cations appears to have a stronger effect on the energy of the HOMO orbital.

3.3. Polyoxotungstate anion-alkali metal cation $[PW_{12}O_{40}]^{3-}[M^+(H_2O)_n]_3$ *ion-pair complexes.*

Following the above preparatory steps, the geometry and electronic structure of the $[PW_{12}O_{40}]^{3-}[M^{+}(H_2O)_{16}]_3$ polyoxotungstates were studied, where M = Li, Na, K, Rb and Cs. With unconstrained energy minimization, the final structures of these complexes were obtained and presented in Figure 7.

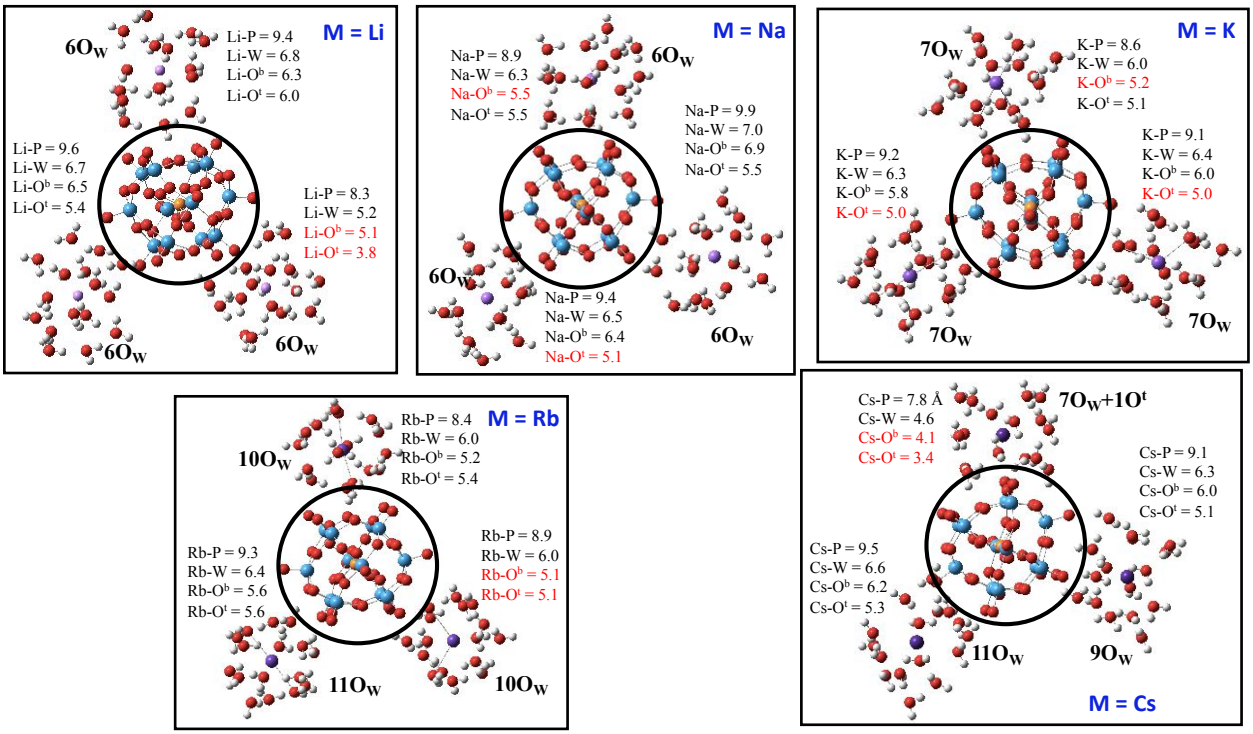

Figure 7. Structures of the $[PW_{12}O_{40}]^{3-}[M^{+}(H_2O)_{16}]_3$ (M=Li, Na, K, Rb, Cs) ion-pair polyoxotungstates. Important distances are given in Å next to each structure, with the shortest ones emphasized in red. The coordination number for each M in the complex is shown in bold as nO_W+mO^t, where O_W is water oxygen and O^t is a terminal oxygen of the POM anion, with n and m being integer.

As seen in Figure 7, the anion/cation complexation motifs in the $[PW_{12}O_{40}]^{3-}[M^{+}(H_2O)_{16}]_3$ polyoxotungstates are similar for all five alkali metals: the cations form a nearly equilateral triangle around the anion $[PW_{12}O_{40}]^{3-}$, with the phosphorus center of the anion being approximately co-planar with the three alkali metal centers. Furthermore, the local structures of the hydrated alkali metal cations closely resemble the corresponding pre-complexation $M^{+}(H_2O)_{16}$ structures. This can be assessed, for example, by the number of coordinated water molecules in the first solvation shell of cation [presented as a pre-complexation/post-complexation numbers: here, (n, m, l) stands for the coordination numbers in the first, second and third $M^{+}(H_2O)_{16}$ cluster], which is found to be (6, 6, 6)/(6, 6, 6), (7, 7, 7)/(6, 6, 6) and (8, 8, 8)/(7, 7, 7) for M = Li, Na and K, respectively. Thus, Li clusters have experienced no change in coordination number, while Na and K clusters each lost one water molecule upon the complexation. For Rb, the number of the coordinated water molecules change as (12, 12, 12)/(10, 10, 11), which could be due to its pre-complex coordination ambiguity. However, for M = Cs, unambiguously, the number of the coordinated water molecules changes as (12, 12, 12)/(7+1, 9, 11), revealing that the Cs-center of the first $Cs^{+}(H_2O)_{16}$ cluster loses 5 water molecules, but gains coordination with the POM anion via its terminal oxygens, and the Cs-centers of the two other $Cs^{+}(H_2O)_{16}$ clusters lose 1 and 3 waters each, respectively.

Consistently, the average M-O^t(POM anion) and M-O^b(anion) bond distances are calculated to be 5.1, 5.4, 5.1, 5.4 and 4.6 Å, and 6.0, 6.3, 5.7, 5.3 and 5.4 for M = Li, Na, K, Rb and Cs, respectively. Based on the above structural analysis, one may conclude that with increase of the atomic number of the alkali metal cation, a solvated $[M^+(H_2O)_{16}$ cluster: (*i*) more readily releases several water molecules from its first coordination sphere, (*ii*) opens additional coordination sites, and (*iii*) interacts stronger with the polyoxometalate anion. As a result, the cation is positioned closer to the POM anion's surface. The calculated binding energy of the hydrated alkali metal cations with the POM anion, defined as $\Delta E = E([PW_{12}O_{40}]^{3-}[M^+(H_2O)_{16}]_3) - E([PW_{12}O_{40}]^{3-}) - 3E(M^+(H_2O)_{16})$ and plotted in Figure 8, alongside a single water dehydration energy of an $M^+(H_2O)_{16}$ pre-complex ion, defined as $\Delta E = E[M^+(H_2O)_{16}] - E[M^+(H_2O)_{15}] - E(H_2O)$, reinforces this conclusion. Indeed, as seen in Figure 8, the $3[M^+(H_2O)_{16}]$-POM binding energy increases (becomes more negative) from M = Li (~ -35 kcal/mol) to M = Cs (~ -55 kcal/mol), while, on the contrary, a single water dehydration energy decreases (becomes less negative) from M = Li (-15.5 kcal/mol) to M = Cs (-0.3 kcal/mol).

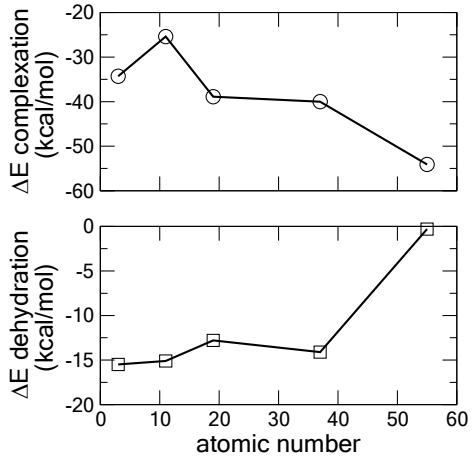

Figure 8. The calculated complexation energy of the $[PW_{12}O_{40}]^{3-}[M^+(H_2O)_{16}]_3$ polyoxotungstates (circles), and the energy of removal of a single water molecule, denoted as "dehydration", from a $M^+(H_2O)_{16}$ ion (squares) for M=Li, Na, K, Rb, and Cs.

Based on the above presented data it is conceivable to characterize the ion-pair complex $[PW_{12}O_{40}]^{3-}[M^+(H_2O)_{16}]_3$ as a "hydrogen bonded" (or "hydrated" ion-pair complex for M = Li, Na and K, but as a "contact" ion-pair complex for M = Rb and Cs. However, as indicated by computation, the transition from the "hydrogen bonded" to the "contact" ion-pairing structures upon change of M via Li, Na, K, Rb, and Cs is a continuous evolution and it is well pronounced in case of light (i.e. Li, Na, and K) and heavy (i.e. Cs) alkali metals. These findings are consistent with available experiments.[5]

As one can expect, the increase of the anion-cation interaction in $[PW_{12}O_{40}]^{3-}[M^+(H_2O)_{16}]_3$ upon going from M = Li to M = Cs would have a well-defined effect on the frontier orbitals of the $[PW_{12}O_{40}]^{3-}$ anion, and consequently, on chemical properties of polyoxometalate. Indeed, an examination of the molecular orbitals of the complex $[PW_{12}O_{40}]^{3-}[M^+(H_2O)_{16}]_3$, which is provided in the Supporting Materials, and comparison with those of the anion $[PW_{12}O_{40}]^{3-}$ shows that both the HOMO and LUMO of $[PW_{12}O_{40}]^{3-}$ are stabilized upon the interaction with $[M^+(H_2O)_{16}]_3$. Importantly, this stabilization effect depends on the nature of the counter cation, and consequently, on the strength of the anion-cation interaction. *Close examination shows that the HOMOs of the $[PW_{12}O_{40}]^{3-}[M^+(H_2O)_{16}]_3$ complexes are not only more strongly stabilized than their LUMO counterparts upon going from M = Li to Cs, but their energies drop below the occupied MOs of the coordinated water molecules.* This effect is more pronounced for the complexes with M = K, Rb and Cs than for M = Li and Na. A full picture of the frontier MOs of the complexes is provided

in Scheme 1, where we qualitatively depict the above discussed observations and show the stabilization trends of the POM-based LUMO/HOMO pairs, and the reverse trend of the water-based HOMOs originating on the hydrated alkali metal clusters.

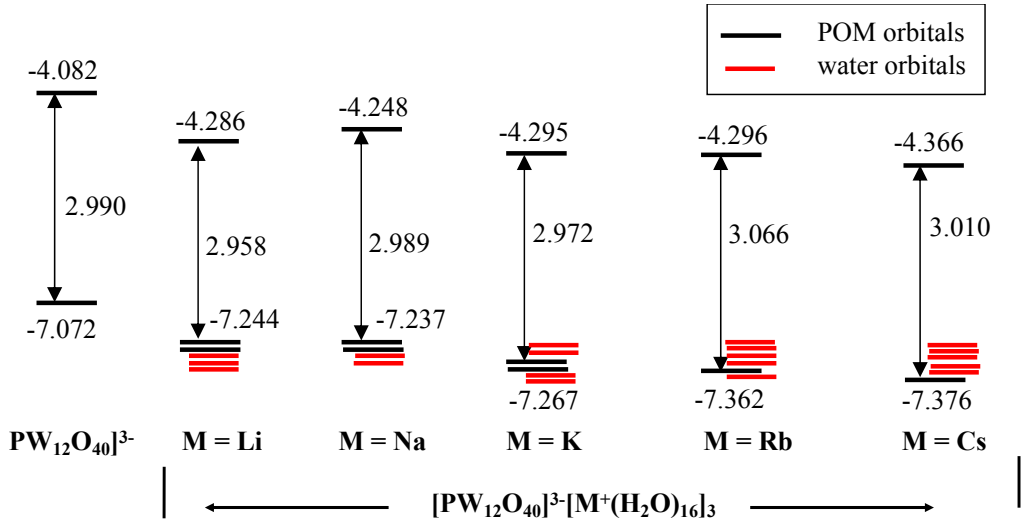

Scheme 1. Schematic illustration of the first few frontier orbitals of $[PW_{12}O_{40}]^{3-}$ and $[PW_{12}O_{40}]^{3-}[M^{+}(H_2O)_{16}]_3$ systems. The HOMO/LUMO pairs localized on the $[PW_{12}O_{40}]^{3-}$ anion are shown by black lines (with the MO and the HOMO-LUMO gap energies provided) and those localized on water by red lines. All energies are given in eV.

As mentioned above, the obvious cause of the HOMO/LUMO stabilization in the $[PW_{12}O_{40}]^{3-}[M^{+}(H_2O)_{16}]_3$ polyoxotungstates is the anion-cation interaction. Here, we find it useful to demonstrate this phenomenon, once again, by deriving a formal correlation of the redox potentials with the energy of complexation. Taking the orbital energies from Scheme 1 and plotting them against the complexation energy reported in Figure 8 yields the plots summarized in Figure 9.

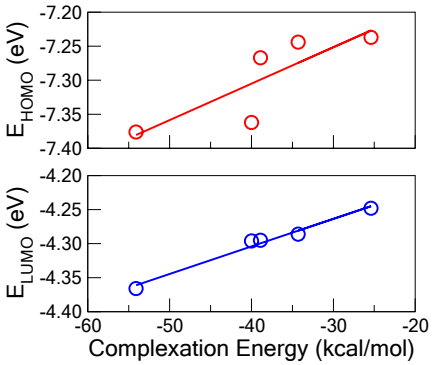

Figure 9. Correlation of the LUMO (E_{LUMO}) and HOMO (E_{HOMO}) energies with the $[PW_{12}O_{40}]^{3-}$ - $[M^{+}(H_2O)_{16}]_3$ complexation energy.

One can infer from the plots a nearly exact linear correlation for E_{LUMO}, with the rate of ~4.1 meV per kcal/mol of complexation, and a less pronounced, yet still arguably linear correlation for E_{HOMO}, with a 5.3 meV per kcal/mol rate of complexation. The less clear linearity of E_{HOMO} can be explained by the fact of HOMO's noticeable spatial mixing with the occupied MOs of water, which causes appreciable perturbation to a simple electrostatically induced stabilization. (This can also be seen in Figure S2 of the Supporting Materials.)

In summary, while anion-cation interaction in the $[PW_{12}O_{40}]^{3-}[M^{+}(H_2O)_{16}]_3$ polyoxotungstates only slightly changes the HOMO-LUMO energy gap, it may significantly impact the chemical properties of the polyoxometalate. Indeed, the POMs with M = Rb and Cs, i.e. the contact ion-pair complexes, can be better electron acceptors than those with M = Li, Na and K, i.e. the hydrogen-

bonded ion-pair complexes. On the contrary, the POMs with M = Rb and Cs are poorer electron donors than those with M = Li, Na and K. Importantly, since the formal HOMOs of the $[PW_{12}O_{40}]^{3-}[M^+(H_2O)_{16}]_3$ polyoxotungstates, with M = Rb and Cs, are the water orbitals, it is conceivable to expect that the first few ionizations of the $[PW_{12}O_{40}]^{3-}[M^+(H_2O)_{16}]_3$ polyoxotungstates will involve ionization of water molecules rather than polyoxotungstate anion.

At this point, we also wish to address the electronic spectra of the $[PW_{12}O_{40}]^{3-}[M^+(H_2O)_{16}]_3$ polyoxotungstates in the visible wavelength range by analyzing the few leading excited singlets. The results of the excited state calculations, partially summarized in Table 1 and more fully in Table S4 of Supporting Materials, show two types of transitions: the O(2*p*)-to-W(5*d*) valence transitions within the polyoxometalate anion, labeled *"intramolecular charge transfer or Intra-CT"*, and the H_2O (π lone-pair)-to-W(5*d*) transitions which we define as charge transfer transitions from solvent to POM anion, labeled *" intermolecular Inter-CT"*. Consistent with the MO picture in Scheme 1, the lowest energy excitations, *i.e.* S_1 states, are *Intra-CT* in character for M = Li and Na, but are *Inter-CT* for M = K, Rb and Cs. The first *Intra-CT* excitations for the complexes with M = K, Rb and Cs appear as S_4, S_{11} and S_{17} states, respectively, lying 0.13, 0.11 and 0.56 eV above their corresponding band origins. In general, as seen in Table 1, all five complexes display much stronger *Inter-CT* than *Intra-CT* characteristics in the long wavelength regime, and that the *Inter-CT* dominance at low energies increases towards the heavier alkali metal cations. Additionally, in the first 17 excited states, the ratio of the number of pure *Inter-CT* states to pure *Intra-CT* or mixed *Intra-CT / Inter-CT* states evolves from Li to Na, K, Rb and Cs as 12:5, 12:5, 13:4, 14:3 and 16:1. It is clear, however, that the addition of more water molecules toward a more realistic bulk solvent representation will dramatically increase these ratios, so that *Inter-CT* character will entirely dominate over POM's *Intra-CT* transitions. *Thus, these calculations show that in the $[PW_{12}O_{40}]^{3-}[M^+(H_2O)_{16}]_3$ polyoxotungstates, with the heavier alkali metal cations, a few leading excitations correlate with the solvent-to-POM (i.e. intermolecular charge transfer, Inter-CT) transitions, rather than with the internal O(2p)-to-W(5d) (i.e. intramolecular charge transfer, Intra-CT) transitions.*

We also should mention that in all $[PW_{12}O_{40}]^{3-}[M^+(H_2O)_{16}]_3$ polyoxotungstates, the leading *Intra-CT* transition is energetically very close to those in the free POM anion (2.98 eV). This result is consistent with the above presented finding that the HOMO-LUMO gap, unlike the individual MO energies, is weakly dependent on the nature of alkali metal cations.

Table 1. Excited state energies (in eV relative to S_0) and dominant orbital character for the first few excited singlets S_n of the $[PW_{12}O_{40}]^{3-}$ anion, and the $[PW_{12}O_{40}]^{3-}[M^+(H_2O)_{16}]_3$ complexes. For the $[PW_{12}O_{40}]^{3-}[M^+(H_2O)_{16}]_3$ systems, "*Inter-CT*" is defined as H_2O(π lone-pair)-to-W(5*d*) charge transfer, and "*Intra-CT*" is defined as the O(2*p*)-to-W(5*d*) valence transition. Some states are approximately evenly mixed *Intra-CT* / *Inter-CT* transitions, labeled here by "*m*" for brevity. By default, unlabeled energies in the columns are "*Inter-CT*".

S_n	$[PW_{12}O_{40}]^{3-}$	M = Li	M = Na	M = K	M = Rb	M = Cs
1	2.984	2.976 (*Intra*)	2.987 (*Intra*)	2.851	2.877	2.423
2	3.031	2.990	3.006	2.897	2.896	2.460
3	3.032	3.024 (*Intra*)	3.015	2.968	2.926	2.769
4	3.054	3.049 (*m*)	3.030	2.980 (*Intra*)	2.934	2.794
5	3.318	3.061 (*m*)	3.034 (*Intra*)	3.012	2.941	2.796
6	3.318	3.081 (*Intra*)	3.036 (*Intra*)	3.013	2.954	2.817

7	3.319	3.132	3.038	3.038 (*Intra*)	2.955	2.831
8	3.329	3.134	3.050	3.051	2.980	2.831
9	3.330	3.188	3.058 (*m*)	3.056	2.982	2.860
10	3.330	3.192	3.062 (*m*)	3.060 (*Intra*)	2.987	2.868
11	3.335	3.203	3.087	3.072 (*Intra*)	2.991 (*Intra*)	2.897
12	3.336	3.211	3.096	3.083	2.999	2.906
13	3.337	3.215	3.144	3.096	3.012	2.919
14	3.386	3.223	3.151	3.128	3.037 (*Intra*)	2.942
15	3.387	3.234	3.152	3.136	3.039	2.954
16	3.388	3.262	3.159	3.140	3.045	2.955
17	3.390	3.264	3.177	3.180	3.070 (*Intra*)	2.986 (*Intra*)

It is important to emphasize that the *Inter-CT* transitions showing up in the low energy part of the spectrum, presented in Figure 10, are relatively dark, compared with the pure POM's strongly active **A** and **B** bands. As seen in Figure 10, where we illustrate the low energy part of the photoabsorption spectra of $[PW_{12}O_{40}]^{3-}[M^{+}(H_2O)_{16}]_3$ polyoxotungstates, the (*Inter-CT)*-sourced absorbance is of the order of 400-600 $L*mol^{-1}*cm^{-1}$, or about two orders of magnitude weaker than (*Intra-CT*)-sourced bands, seen in Figure 3. Despite the strong dipole change component arising due to the charge transfer between water and the POM, the quantum mechanical factor, which depends on the involved orbital spatial overlaps, is extremely small, making the *Inter-CT* transitions dark. (The orbitals relevant to the involved *Inter-CT* transitions are provided in the SI for visual inspection.) From Figure 10 one may also see that the long wavelength tail of the spectrum is much more pronounced in the Cs complex than in the other four. This effect is due to the higher density of *Inter-CT* states of the Cs complex, as well as to its S_1 and S_2 states, which are both substantially lower, by ~0.4-0.5 eV, than their *Inter-CT* counterparts in the other complexes.

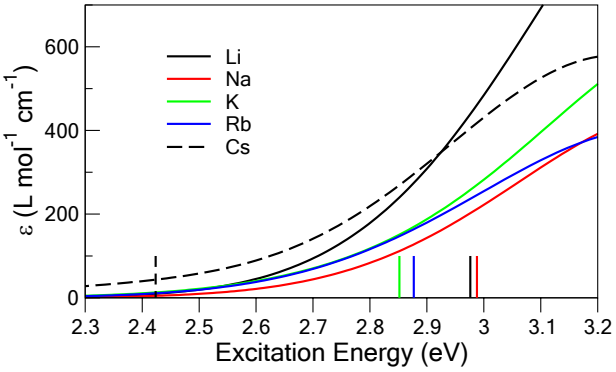

Figure 10. The low energy part of the photo-absorption spectra of POM/counter cation complexes, dominated by *Inter-CT* transitions, convoluted with gaussians using the data reported in Tables 1 and S4. The vertical sticks mark the corresponding band origin for each of the five complexes.

4. Concluding remarks

The impetus for this study was to understand the geometric structure, electronic structure and chemical properties of the hydrated alkali-metal Keggin heteropolytungstates. We have used density functional theory to elucidate the impact of fully hydrated (with sixteen water molecules) alkali-metal counter cation on the electronic and geometry structures of the phosphotungstate acid. The calculations show that:

1. the HOMO of the free anion $[PW_{12}O_{40}]^{3-}$ is a linear combination of the 2*p* AOs of the bridging oxygens, and the first few LUMOs are the 5*d* orbitals of the tungsten atoms of the Keggin

polyanion. The lowest energy electron excitations, *i.e.* the $S_0 \rightarrow S_1$ excitation, are near 3 eV, corresponding to the O(2*p*) → W(5*d*) transitions.

2. The first solvation shell of the Li^+, Na^+, K^+, Rb^+, and Cs^+ cations contains a maximum of 6, 7, 8, 10-12, and 12 closely coordinated water molecules, respectively. The HOMOs of the $M^+(H_2O)_n$ clusters are 2*p* orbitals of the water molecules located in the second solvation shell of metal cations, while the LUMOs of these clusters are 2*p*σ* orbitals which are delocalized over the entire water body of the $M^+(H_2O)_n$ clusters. The occupied MOs of the waters in the first solvation shell are spatially closer to the alkali metal cations and are stabilized the most by the cation-water interactions.
3. Upon anion/cation complexation to form $[PW_{12}O_{40}]^{3-}[M^+(H_2O)_{16}]_3$ polyoxotungstates, the $M^+(H_2O)_{16}$ clusters undergo the following structural changes. With an increase in the atomic number of the alkali metal cation, the cluster: (*i*) releases several water molecules from its first coordination sphere, (*ii*) opens coordination sites, and (*iii*) interacts strongly with polyoxometalate anion via its terminal oxygen centers. Here, the complex $[PW_{12}O_{40}]^{3-}[M^+(H_2O)_{16}]_3$ is characterized as a "hydrogen bonded" ion-pair complex for M = Li, Na and K, but as a "contact" ion-pair complex for M = Rb and Cs. This conclusion is consistent with the limited experimental data.[5]
4. The anion-cation interaction in the $[PW_{12}O_{40}]^{3-}[M^+(H_2O)_{16}]_3$ polyoxotungstates only slightly affects the HOMO-LUMO energy gap, while it may significantly impact the chemical properties of the polyoxometalate. Indeed, because of the strong anion-cation interaction, the "contact" ion-pair complexes with M = Rb and Cs become better electron acceptors than the "hydrogen-bonded" ion-pair complexes with M = Li, Na and K. Importantly, since HOMOs of the $[PW_{12}O_{40}]^{3-}[M^+(H_2O)_{16}]_3$ polyoxotungstates, with M = Rb and Cs, are water-based orbitals, it is conceivable to expect that the first few ionizations of the $[PW_{12}O_{40}]^{3-}[M^+(H_2O)_{16}]_3$ polyoxotungstates will involve water molecules rather than the polyoxotungstate anion.
5. The electronic excitations in the visible part of the electronic absorption spectrum of these ion-pair complexes are predominantly solvent-to-POM (i.e. intermolecular) charge transfer in character. The number of intermolecular charge-transfer excited states in the visible part of the electronic absorption spectrum of these ion-pair complexes increases with the increasing atomic number of the alkali metals.

Conflicts of interest

There are no conflicts to declare.

Corresponding Author:
D. G. Musaev, e-mail: dmusaev@emory.edu

ACKNOWLEDGEMENTS

This work was funded by the U.S. Department of Energy, Office of Basic Energy Sciences, Solar Photochemistry Program (DE-FG02-07ER-15906). The authors gratefully acknowledge NSF MRI-R2 grant (CHE-0958205 for D. G. M.) and the use of the resources of the Cherry L. Emerson Center for Scientific Computation.

REFERENCES

1. M. T. Pope, *Heteropoly and Isopoly Oxometalates*, Springer-Verlag, Berlin, 1983.
2. V. W. Day, W. G. Klemperer, *Science,* 1985, **228**, 533.
3. M. T. Pope, A. Müller, *Angew. Chem. Int. Ed.,* 1991, **30**, 34.
4. D.-L. Long, R. Tsunashima, L. Cronin, L., *Angew. Chem. Int. Ed.,* 2010, **49**, 1736.
5. A. Misra, K. Kozma, C. Streb, M. Nyman, *Angew. Chem. Int. Ed.,* 2020, **59**, 596.
6. M. Kozik, L. C. W. Baker, *J. Am. Chem. Soc.,* 1987, **109**, 3159.
7. M. Kozik, L. C. W. Baker, *J. Am. Chem. Soc.,* 1990, **112**, 7604.
8. P. Carloni, L. Eberson, *Acta Chem. Scand.,* 1991, **45**, 373.
9. J. F. Kirby, L. C. W. Baker, *Inorg. Chem.,* 1998, **37**, 5537.
10. V. A. Grigoriev, C. L. Hill and I. A. Weinstock, *J. Am. Chem. Soc.,* 2000, **122**, 3544.
11. V. A. Grigoriev, D. Cheng, C. L. Hill, I. A. Weinstock, *J. Am. Chem. Soc.,*2001, **123**, 5292.
12. T. W. Swaddle, *Chem. Rev.,* 2005, **105**, 2573.
13. A. Czap, N. I. Neuman, T. W. Swaddle, *Inorg. Chem.,* 2006, **45**, 9518.
14. T. Okuhara, N. Mizuno, M. Misono, *Adv. Catal.,* 1996, **41**, 113.
15. J. B. Moffat, *Metal-Oxygen Clusters: The Surface and Catalytic Properties of Heteropoly Oxometalates,* Kluwer Academic/Plenum Publishers, New York, 2001.
16. I. V. Kozhevnikov, *Chem. Rev.,* 1998, **98**, 171.
17. N. Mizuno, M. Misono, *Chem. Rev.,* 1998, **98**, 199.
18. C. P. Pradeep, D.-L. Long, L. Cronin, *Dalton Trans.,* 2010, **39**, 9443.
19. G. J. T. Cooper, A. G. Boulay, P. J. Kitson, C. Ritchie, C. J. Richmond, J. Thiel, D. Gabb, R. Eadie, D.-L. Long, L. Cronin, *J. Am. Chem. Soc.,* 2011, **133**, 5947.
20. M. R. Antonio, M. Nyman, T. M. Anderson, *Angew. Chem. Int. Ed.,* 2009, **48**, 6136.
21. J. M. Clemente-Juan, E. Coronado, A. Gaita-Arino, *Chem. Soc. Rev.,* 2012, **41**, 7464.
22. J. T. Rhule, C. L. Hill, D. A. Judd, R. F. Schinazi, *Chem. Rev.,* 1998, **98**, 327.
23. W. H. Knoth, R. L. Harlow, *J. Am. Chem. Soc.,* 1981, **103**, 1865.
24. A. Müller, E. Beckmann, H. Bögge, M. Schmidtmann, A. Dress, *Angew. Chem.,* 2002, **114**, 1210.
25. G. M. Brown, M. R. Noe-Spirlet, W. R. Busing, H. A. Levy, *Acta. Cryst. B,* 1977, **B33**, 1038.
26. X. Zhang, Q. Chen, D. C. Duncan, C. Campana, C. L. Hill, *Inorg. Chem.,* 1997, **36**, 4208.
27. Y. Zhao, D. G. Truhlar, *J. Chem. Phys.,* 2006, **125**, 194101.
28. R. C. Chapleski Jr., D. G. Musaev, C. L. Hill, D. Troya, *J. Phys. Chem. C,* 2016, **120**, 16822.
29. A. L. Kaledin, D. Driscoll, D. Troya, D. Collins-Wildman, C. L. Hill, J. Morris, D. G. Musaev, *Chem. Sci.,* 2018, **9**, 2147.
30. V. A. Rassolov, M. A. Ratner, J. A. Pople, P. C. Redfern, L. A. Curtiss, *J. Comp. Chem.,* 2001, **22**, 976.
31. T. H. Dunning Jr. and P. J. Hay, in *Modern Theoretical Chemistry vol. 3*, ed. H. F. Schaefer III, Plenum, New York, 1977.
32. P. J. Hay, W. R. Wadt, *J. Chem. Phys.,* 1985, **82**, 270.
33. R. Bauernschmitt, R. Ahlrichs, *Chem. Phys. Lett.,* 1996, **256**, 454.
34. J. Tomasi, B. Mennucci, R. Cammi, *Chem. Rev.,* 2005, **105**, 2999.

35. G. Scalmani, M. J. Frisch, B. Mennucci, J. Tomasi, R. Cammi and V. Barone, *J. Chem. Phys.,* 2006, **124**, 094107.
36. M. J. Frisch, G. W. Trucks, H. B. Schlegel, G. E. Scuseria, M. A. Robb, J. R. Cheeseman, G. Scalmani, V. Barone, B. Mennucci, G. A. Petersson, H. Nakatsuji, M. Caricato, X. Li, H. P Hratchian, A. F. Izmaylov, J. Bloino, G. Zheng, J. L. Sonnenberg, M. Hada, M. Ehara, K. Toyota, R. Fukuda, J. Hasegawa, M. Ishida, T. Nakajima, Y. Honda, O. Kitao, H. Nakai, T. Vreven, J. A. Montgomery Jr, J. E. Peralta, F. β. Ogliaro, M. J. Bearpark, J. Heyd, E. N. Brothers, K. N. Kudin, V. N. Staroverov, R. Kobayashi, J. Normand, K. Raghavachari, A. P. Rendell, J. C. Burant, S. S. Iyengar, J. Tomasi, M. Cossi, N. Rega, N. J. Millam, M. Klene, J. E. Knox, J. B. Cross, V. Bakken, C. Adamo, J. Jaramillo, R. Gomperts, R. E. Stratmann, O. Yazyev, A. J. Austin, R. Cammi, C. Pomelli, J. W. Ochterski, R. L. Martin, K. Morokuma, V. G. Zakrzewski, G. A. Voth, P. Salvador, J. J. Dannenberg, A. Dapprich, A. D. Daniels, ñ. n. Farkas, J. B. Foresman, J. V. Ortiz, J. Cioslowski, D. J. Fox, Gaussian, Inc., Wallingford, CT, USA, 2009.
37. T. Okuhara, N. Mizuno, M. Misono, *Advances in Catalysis*, 1996, **41**, 113.
38. (a) X. Lopez, J. J. Carbo, C. Bo, J. M. Poblet, "Structure, properties and reactivity of polyoxometalates: a theoretical perspective" *Chem. Soc. Rev.*, **2012**, 41, 7537; (b) X. Lopez, J. M. Maestre, C. Bo, J. M. Poblet, "Electronic properties of polyoxometalates: A DFT study of α/β-$[XM_{12}O_{40}]^{n-}$ relative stability (M= W, Mo and X a main group element)", *J. Am. Chem. Soc.,* 2001, **123**, 9571; (c) J. M. Maestre, X. Lopez, C. Bo, J. M. Poblet, N. Casan-Pastor, " Electronic and magnetic properties of α-keggin anions: A DFT Study of $[XM_{12}O_{40}]^{n-}$,(M= W, Mo; X= Al^{III}, Si^{IV}, P^{V}, Fe^{III}, Co^{II}, Co^{III}) and $[SiM_{11}VO_{40}]^{m-}$ (M= Mo and W)", *J. Am. Chem. Soc.*, 2001, **123**, 3749; (d) X. Lopez, C. Nieto-Draghi, C. Bo, J. B. Avalos, J. M. Poblet, "Polyoxometalates in solution: molecular dynamics simulations on the α-PW12O403-Keggin anion in aqueous media", *J. Phys. Chem. A*, 2005, **109**, 1216.
39. H. Lv, Y. V. Geletii, C. Zhao, J. W. Vickers, G. Zhu, Z. Luo, J. Song, T. Q. Lian, D. G. Musaev, C. L. Hill, „Polyoxometalate water oxidation catalysts and the production of green fuel," *Chem. Soc. Rev.*, 2012, **41**, 7572.
40. I. D. Brown, *The Chemical Bond in Inorganic Chemistry: The Bond Valence Model*, Oxford University Press, Oxford, 2002.
41. P. Wang, R. Shi, Y. Su, L. Tang, X. Huang, J. Zhao, *Frontiers in Chemistry,* 2019, **7**, 1.
42. G. N. Merrill, S. P. Webb, D. B. Bivin, *J. Phys. Chem. A,* 2003, **107**, 386.
43. D. Feller, *J. Phys. Chem. A,* 1997, **101**, 2723.

Table of Contents

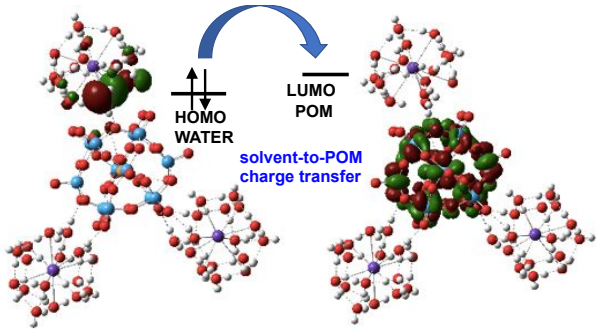

The $[PW_{12}O_{40}]^{3-}[M^{+}(H_2O)_{16}]_3$ is a "hydrogen bonded" ion-pair complex for M = Li, Na and K, but is a "contact" ion-pair complex for M = Rb and Cs, *Intermolecular charge transfer from the solvated counter cations* $M^{+}(H_2O)_{16}$ *to the anion* $[PW_{12}O_{40}]^{3-}$.

Table of Contents

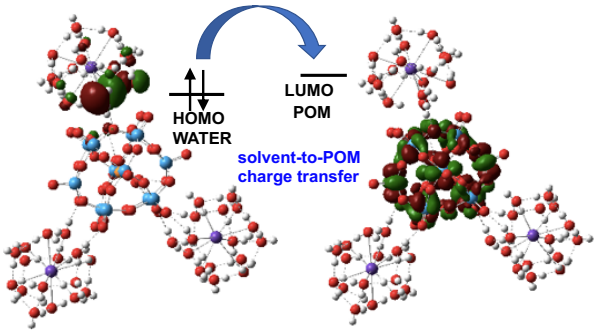

The $[PW_{12}O_{40}]^{3-}[M^{+}(H_2O)_{16}]_3$ is a "hydrogen bonded" ion-pair complex for M = Li, Na and K, but is a "contact" ion-pair complex for M = Rb and Cs, *Intermolecular charge transfer from the solvated counter cations* $M^{+}(H_2O)_{16}$ *to the anion* $[PW_{12}O_{40}]^{3-}$.